AAPS PharmSciTech, Vol. 10, No. 2, June 2009 (© 2009)
DOI: 10.1208/s12249-009-9239-9

Research Article

Modulation and Optimization of Drug Release from Uncoated Low Density Porous Carrier Based Delivery System

Praveen Sher,[1,2,4] Ganesh Ingavle,[2] Surendra Ponrathnam,[2] Pankaj Poddar,[3] and Atmaram P. Pawar[1,4]

Received 14 August 2008; accepted 9 April 2009; published online 8 May 2009

Abstract. The purpose of this research work was to explore an application of uncoated porous drug carrier prepared by single-step drug adsorption for a delivery system based on integration of floating and pulsatile principles intended for chronotherapy. This objective was achieved by utilizing 3^2 factorial design, solvent volume (X_1) and drug amount (X_2) as selected variables, for drug adsorption using solvents, methanol, and dichloromethane (DCM), of varying polarity. Nitrogen adsorption (N_2), scanning electron microscopy of cross-sections, and atomic force microscopy were done to study adsorption patterns and their effect on release pattern. Drug release study was customized by performing for 6 h in acidic environment to mimic gastroretention followed by basic environment akin to transit phase. Correlation between porous data from mercury and N_2 adsorption was probably studied for the first time. Observed regression analysis values for pore volume, surface area, and drug release indicated the influence of selected variables. Total release range in acidic medium was 12.77–24.57% for methanol, 8.79–15.26% for DCM, and final release of 69.45–92.23% for methanol, and 60.16–99.99% for DCM influenced by varying internal geometries was observed. Present form of drug delivery system devoid of any additives/excipients influencing drug release shows distinct behavior from other approaches/technologies in chronotherapy by (a) observing desired low drug release (8%) in acidic medium, (b) overcoming the limitations of process variables caused by multiple formulation steps and different characteristic polymers, (c) reducing time consumption due to single step process, and (d) extending as controlled/extended release.

KEY WORDS: chronotherapy; floating pulsatile drug delivery system; low density porous carrier; pore data; solvent polarity.

INTRODUCTION

During the past decade, there has been an exponential growth in the investigations related to the application of porous material in controlling temporal or distributional drug release by oral, pulmonary, transdermal, and injectables routes. Inherent attractive features, like stable uniform porous structure, high surface area, tunable pore sizes with narrow distribution, and well-defined surface properties, make them suitable for their inclusion in any form of delivery system. Porous network, characteristic of an individual material, is important in determining both natural and practical applications such as adsorption, dissolution, and diffusion of drugs. This allows them to adsorb drugs and release them in a more reproducible and predictable manner. Until today, different types of drugs with small and large molecular size have been evaluated (1–6). Various methods like stirring in drug solution or suspension, immersion for long times until equilibrium is reached, vacuum, emulsion formation, gravimetric method, and solvent evaporation to entrap the drug within the carrier are reported (6–11).

In our previous communications, we had demonstrated the applications of a porous carrier, Accurel MP 1000®, made of isotactic polypropylene, as an uncoated drug carrier (12) and its utility for the development of 'floating pulsatile drug delivery system' intended for chronotherapy (13). This therapy, based on circadian rhythm, is contrary to principles of present delivery systems based on providing variable/constant drug amount over a period of time, where timed non-uniform release profile is found more beneficial than a uniform one (14).The essential features of this conceptual delivery system exhibit as a (a) multiparticulate system, (b) combination of gastroretentive and pulsatile principles in same dosage form, (c) single-step formulation process using low-density porous carrier as drug-loading core, (d) idealistic drug release profile that is effective at morning time intended for a particular pathological condition based on chronotherapy, and (e) having low drug release in stomach suited for non-steroidal anti inflammatory drug (NSAID) class of drug (ibuprofen).

The contribution of low-density porous carrier in the development of this drug delivery system associates major significance by (a) ensuring the retention of dosage form in

[1] Department of Pharmaceutics, Poona College of Pharmacy and Research Centre, Bharti Vidyapeeth University, Erandwane, Pune, 411038, Maharashtra State, India.
[2] Polymer Science and Engineering Division, National Chemical Laboratory, Pune, 411008, India.
[3] Nanoscience Group, Material Chemistry Division, National Chemical Laboratory, Pune, 411008, India.
[4] To whom correspondence should be addressed. (e-mail: p_atmaram @rediffmail.com; sherpraveen@gmail.com)

the stomach for an extended period without using any excipients for enhancing floating, (b) simultaneous least release all through this period (resembling lag phase) suited for NSAID drugs to avoid gastric irritation, (c) choice of drug loading (melt and solvent evaporation), and(d) limit/overcome various formulation variables by acting as a drug-loading core using single formulation step when compared with other approaches/methods, which need multiple steps by using various polymers and excipients to achieve such release profile. The implication of last point seem to be realistic not only when compared with our previous reported work using hydrogels for formulating the same delivery system (15) but also with other methods based on different approaches (10,16–20) and technologies like OROS®, CONTIN®, CEFORM®, TIMERx®, etc. (21) developed for chronotherapy.

Successful relevance of formulating this conceptual system reported earlier was done by using just three batches via melt and solvent evaporation method (13). Based on excellent observed results, the need to study/explore further drug adsorption via solvent evaporation for its simplicity along with optimization by employing factorial design was considered, thereby stating as the objective of present work. The same design of experiment was used earlier in another study for ascertaining as a drug carrier, which in turn acted as a source of comparison for understanding various aspects of mass transfer (12). Additional characterization process by drift Fourier transform infrared analysis (FTIR), scanning electron microscopy (SEM) of cross-sectional areas, N_2 adsorption, and atomic force microscopy (AFM) was done for better understanding. First attempt to find any correlation between porosimetry data obtained from N_2 adsorption by Brunauer–Emmett–Teller (BET) method and mercury porosimetry (12) for drug-loaded porous carrier was done. Drug release study was tailored for 6 h as the maximum gastric floating time to evaluate the concept of floating followed by 3 h in basic medium.

MATERIAL AND METHODS

Materials

Accurel MP 1000® (Membrana ,Germany), a low-density microporous polypropylene microparticles with particle size <1,500 μm, pore size in the range from 5 to 20 μm, and void volume of 70% and ibuprofen (Cipla, India) were obtained as a generous gift. Methanol (M), dichloromethane (DCM), and other reagents were of analytical grade.

Preparation of Drug-Loaded Beads

Drug Loading

Ibuprofen was loaded onto the porous beads by solvent evaporation. Accurel MP 1000 was closely sieved in the range of 250–350 μm to nullify effect due to variation in particle size. In a typical study, various amounts of drug was dissolved in the multiple volumes of solvent (M or DCM) followed by the constant addition of 100 mg Accurel MP 1000 ®, kept to evaporate solvent under ambient conditions.

Factorial Design

A 3^2 design was employed to find the interaction between the selected variables. The variables chosen were volume of solvent (X_1) and the amount of drug (X_2) at three different levels. The coded and the actual values of the experimental design are given in Table I. The data analysis of values obtained for pore volume, surface area, pore diameter, and drug release at various intervals from all batches were subjected to multiple regression analysis using statistical software Unistat® (Statistic version 3, Meglon, USA). The equation fitted was

$$Y = \beta_0 + \beta_1 X_1 + \beta_2 X_2 + \beta_{11}X_1^2 + \beta_{22}X_2^2 + \beta_{12}X_1X_2$$

where Y=measured response, X=levels of factors, and β= coefficient computed from the responses of the formulations.

Evaluation and Characterization of Microparticles

Yield and Drug Content

The dried weight of microparticles after drug loading was recorded as final yield. The drug-loaded beads were dissolved in methanol kept on ultrasonicator, and the content of drug content was assayed by determining (in triplicate) the absorption at 221 nm using UV-VIS Spectrophotometer V-500 (Jasco International Co. Ltd., Japan). The experiment was repeated thrice in order to establish accuracy and precision of the method.

Table I. Experimental Variables of Factorial Design with Their Coded Levels and Actual Values Yield and Drug Content

Batch	Coded levels [solvent (X_1), drug (X_2)]	Solvent (ml) (X_1)	Drug (mg) (X_2)	Practical yield (%)		Drug content (%)	
				m	d	m	d
1	−1,−1	1	100	95.0±1.21	97.17±1.33	85.43±2.31	100±0.16
2	−1,0	1	200	87.33±0.86	98.52±1.65	85.85±2.65	100±0.21
3	−1,1	1	300	83.50±1.34	98.98±1.36	82.74±3.21	100±0.50
4	0,−1	3	100	98.35±1.24	89.88±1.32	79.90±1.21	94.63±1.56
5	0,0	3	200	93.56±1.23	91.26±1.41	86.37±1.32	99.25±1.37
6	0,1	3	300	89.63±1.14	96.50±1.33	86.20±1.32	92.7±1.58
7	1,−1	5	100	95.62±1.56	92.50±1.20	81.16±2.30	99.25±1.09
8	1,0	5	200	89.50±1.33	92.12±2.00	83.27±1.01	97.70±1.54
9	1,1	5	300	88.00±1.61	91.23±0.65	89.26±1.02	93.52±1.07

m methanol, *d* DCM

Differential Scanning Calorimetry

Thermograms of ibuprophen and Accurel MP 1000 microparticles with and without drug were obtained using differential scanning calorimeter (Mettler-Toledo DSC 821^e, Switzerland) equipped with an intracooler. Indium standard was used to calibrate the temperature and enthalpy scale. The powder samples were hermetically sealed in perforated aluminum pans and heated at constant rate of 10°C/min over the temperature range 25–150°C. The system was purged with nitrogen gas at the rate of 100 mL/min to maintain inert atmosphere.

X-ray Powder Diffraction

X-ray powder diffraction (XRD) patterns of drug and Accurel MP 1000® beads with and without drug were recorded by using an X-ray diffractometer (Philips PW 1729, The Netherlands). Samples were irradiated with monochromatized Cu K_α radiation (1.542 Å) and analyzed at 2θ between 2° and 60°. The voltage and current used were 30 kV and 30 mA, respectively. The range and the chart speed were 5×10^3 CPS and 10 mm/2θ, respectively.

Thermogravimetric Analysis

Appropriately weighed drug-loaded microparticles were subjected to gravimetric assay between 35 and 175°C, with the heat flow of 5°C/min using Thermogravimetric Instrument (Seiko TG/DTA-32, Japan). All experiments were performed in the presence of static air.

Fourier Transform Infrared Analysis

FTIR measurements of drug, Accurel MP 1000®, and drug-loaded ones were obtained on FTIR spectrophotometer (Spectrum One, Perkin Elmer Instruments, UK). Samples were prepared by mixing with KBr and placing in the sample holder. The spectra were scanned over the wave number range of 3,600 to 400 cm^{-1} at ambient temperature.

Surface Topography

Microphotographs of the cross-sections of beads were observed using scanning electron microscope (Cambridge Stereoscan 120, UK) operated with an acceleration voltage of 10 kV. The beads were mounted on the standard specimen mounting stubs and were coated with a thin layer (20 nm) of gold in sputter coater unit (VG Microtech, UK).

Atomic Force Microscopy

AFM measurements were performed in ambient condition on coated pellets without any further sample preparation. The AFM measurements were performed repeatedly on many different pellets and on several different areas. Although variations were seen, the images presented were typical of those most frequently observed. All the AFM measurements were done in the contact mode using a commercial Multimode with Nanoscope® IV controller (Veeco Instruments Inc., Santa Barbara, CA, USA). Height and deflection images were taken and analyzed using the NanoScope version 5.12r5 software in the offline mode.

Porosity Measurement

Total surface area and the porosity of the Accurel MP 1000® microparticles with and without drug were measured by nitrogen adsorption using a porosimeter (Quantachrome instrument, Autosorb-1^{TM}, gas sorption system, Ontario, Canada). Briefly, weighed amounts of samples were placed in the glass cells and outgassed with nitrogen at 25°C for 3 h before analysis. Subsequently, the sample and the reference cells were immersed in liquid nitrogen at −196°C, and absorption isotherm was obtained from the volume of nitrogen (cm^3/g) adsorbed onto the surface as a function to relative pressure. Total surface area was calculated by BET method. Various evaluation parameters were obtained by using Autosorb-1^{TM} software. Mercury intrusion porosimetry was done using Mercury porosimeter (Autoscan 33 USA). Samples were first loaded with mercury in a pressurized cell under vacuum and later subjected to pressure range of 0–33,000 psi (12).

Dissolution Release Studies

The dissolution of drug-loaded Accurel MP 1000 ® beads was studied using USP XXIV type II dissolution test apparatus (Electrolab TDT-06P, India), containing 900 mL of

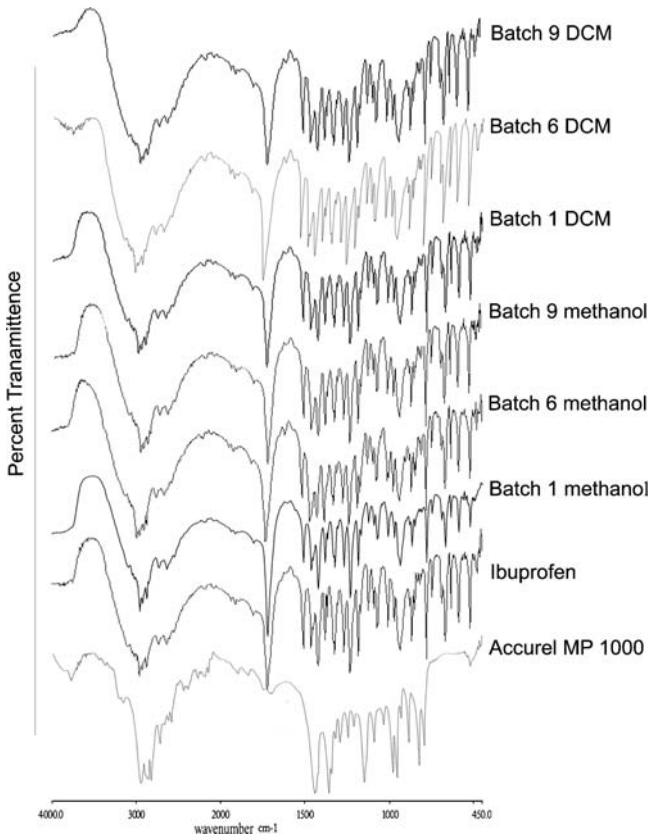

Fig. 1. FTIR spectra of Accurel MP 1000 microparticles, drug and different batches

pH 1.2 HCl and pH 7.2 phosphate buffer maintained at 37± 0.5°C and stirred at 100 rpm for 6 and 3 h, respectively. Samples were collected periodically and replaced with a fresh dissolution medium. Data were analyzed using PCP Disso software (v2.08, Poona College of Pharmacy, India). All readings were made in triplicate.

Stability Studies

The stability of few selected drug-loaded Accurel MP 1000® batches was monitored up to 3 months at ambient temperature and relative humidity (30°C/60% RH). Samples were removed and characterized by dissolution studies and DSC.

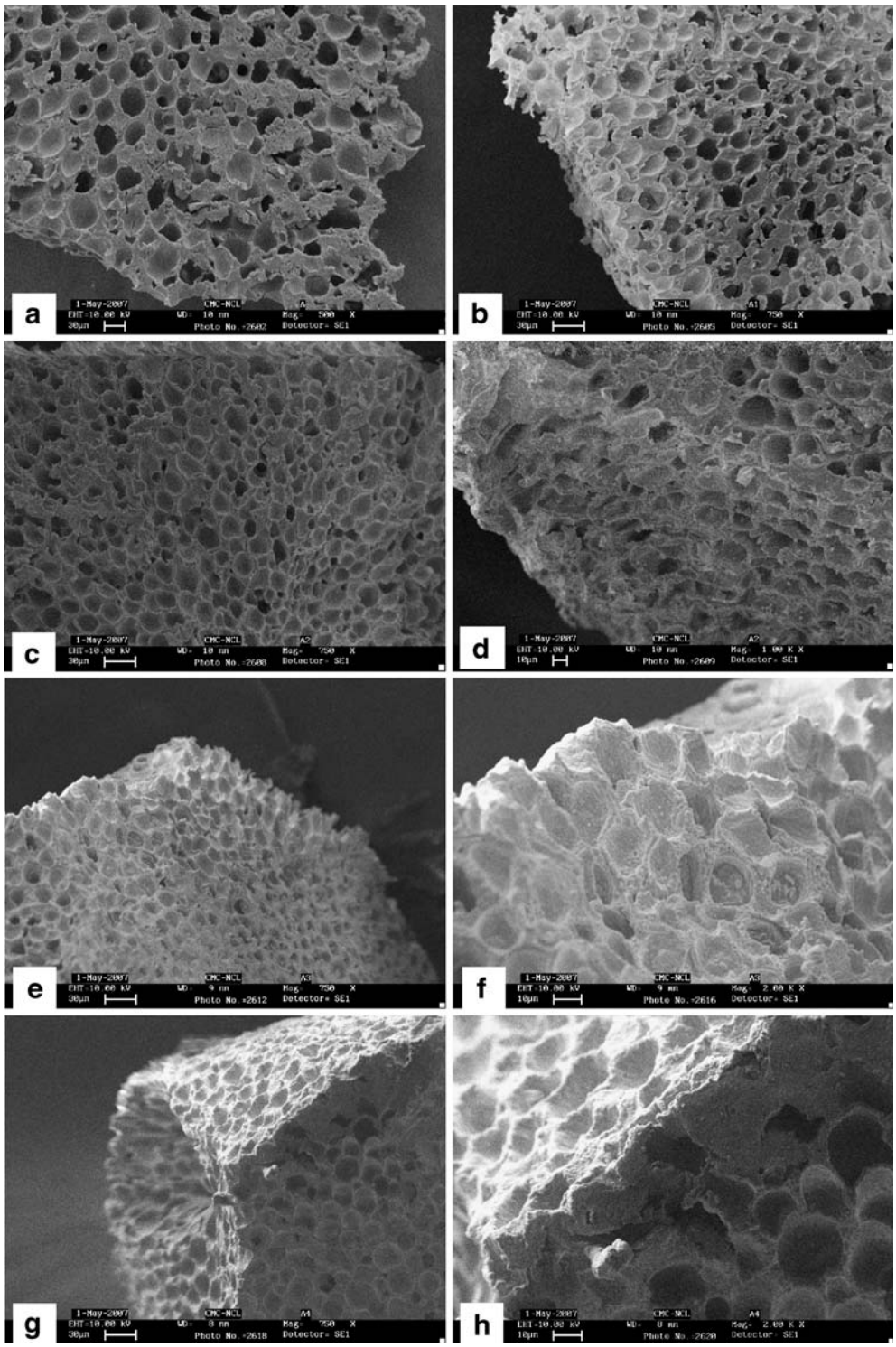

Fig. 2. SEM of **a** Accurel MP 1000 microparticles (×500), **b** batch 4 methanol (×750), **c** (×750) and **d** (×1.00K) batch 6 methanol, **e** (×750) and **f** (×2.0K) batch 4 DCM, **g** (×750) and **h** (×2.0K) batch 6 DCM

RESULTS AND DISCUSSION

The observed values for yield and drug content are given in Table I. Summary of the earlier reported results entail the influence of solvent nature, volumes, and drug amount on the observed values, which was well supported by statistical analysis. DSC and XRD predicted no change in crystalline nature during adsorption. Influence of pore shielding effect using different solvents suggesting discreet drug adsorption was observed by TGA.

Evaluation of Drug-Loaded Microparticles

FTIR results are displayed in Fig. 1. Peak values from 2,961 to 2,722 cm^{-1} of Accurel MP 1000® showing multiple peaks transformed in to sharp triplet peaks after drug adsorption without changing the values of other peaks like 2955, 2922, 2869 cm^{-1} so on. Same was true for particular drug peaks, which show perfect repetition in the range of 1,507 to 2,173 cm^{-1}. Apart from them, various other peaks also showed excellent reproducibility. Another characteristic peaks around 2,625 and 2,730 cm^{-1} indicated toward the dimmer formation signifying the interaction of drug over the hydrophobic surface (22). Overall, these results suggest the physical nature of interaction rather than chemical one.

Surface Characteristics of Drug-Loaded Microparticles

In the pursuit of studying inner/core adsorption behavior for descriptive follow-up, SEM of cross-sections of the microparticles was considered as shown in Fig. 2. Regular spread out adsorption pattern using methanol was observed in Fig. 2b–d. This can be related to lower viscosity and slow phase transformation caused by high boiling point of solvent. At low solvent volume, the drug adsorption is slightly concentrated in upper layers, which change with increasing solvent volume by showing migration toward the core as seen in Fig. 2c and d. This demonstrates the interactive and mobile behavior of drug, having both hydrophilic and hydrophobic segments, over hydrophobic polypropylene surface, whereas polar interactions take place between adsorbed molecules of methanol and those in the solution resulting in observed adsorption orientation. The magnitude of these interactions can show dependence upon free energy of solid and the dispersed adsorbate (22). On the contrary, DCM, having low boiling with low polarity, indicating fast phase change, depicts exactly an opposite pattern than observed with methanol (Fig. 2e–h). These characteristic pictures reveal the concentric adsorption at the surface in the form of stakes running throughout. The partial migration can be due to the decreased polarity of solvent limiting wetting of hydrophobic surface (23). Higher magnification reveal the hemispherical adsorption behavior reported earlier using less polar solvent with hydrophobic surface (24).

AFM was done for further evaluation of the surface morphology for any difference in adsorption pattern as seen in Figs. 3 and 4. A contact mode AFM measurement of batch 7 using methanol in air was observed (Fig. 3a–f). All the corresponding images and 3D plot suggest the true character of the surface. The surface shows wavy nature, which is indicated by the light and dark colors in the images, having irregular patterns caused by depressions and counters. Pictures revealed cracks and height conditions of around 1 μm with a non-regular pattern. Cracks were found even at high magnifications, which suggest the discontinuity of the adsorbed drug layer. This type of surface may be due to the underlying texture of the core structure and/or due to various drying phenomenon occurring during solvent evaporation governed by capillary and diffusion (25). Other factor that surfaced can be due to the interactions taking place using

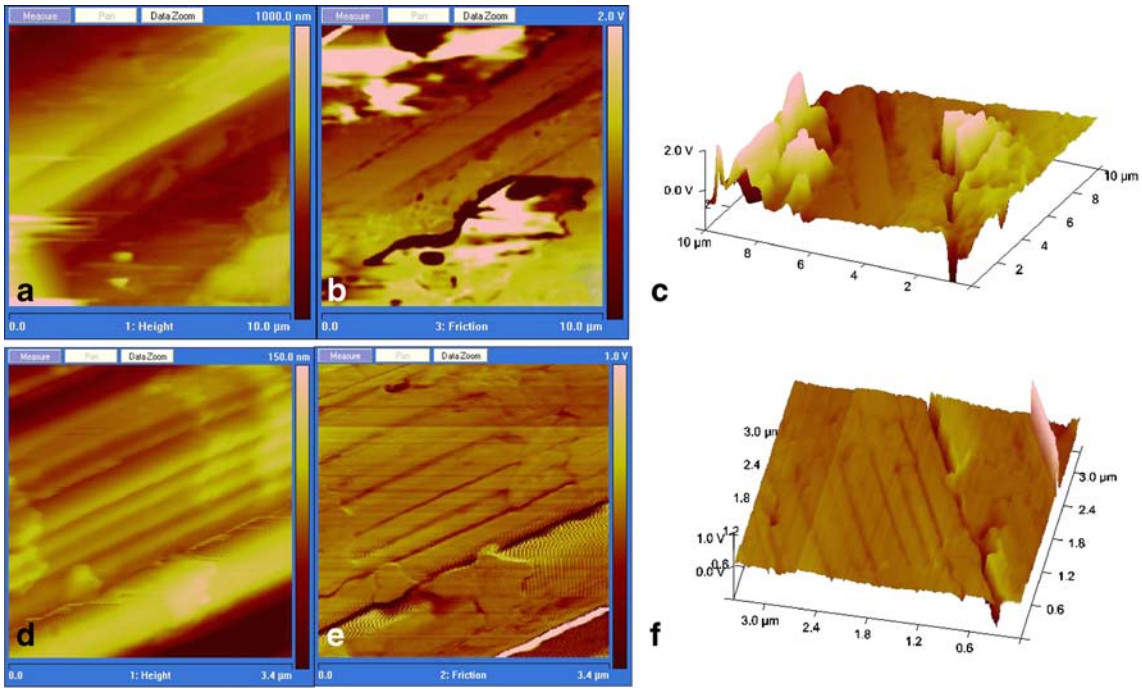

Fig. 3. AFM figures of batch 7 methanol: **a** height, **b** friction, **c** 3D graph for 10 μm, **d** height, **e** friction, **f** 3D graph for 3.4 μm

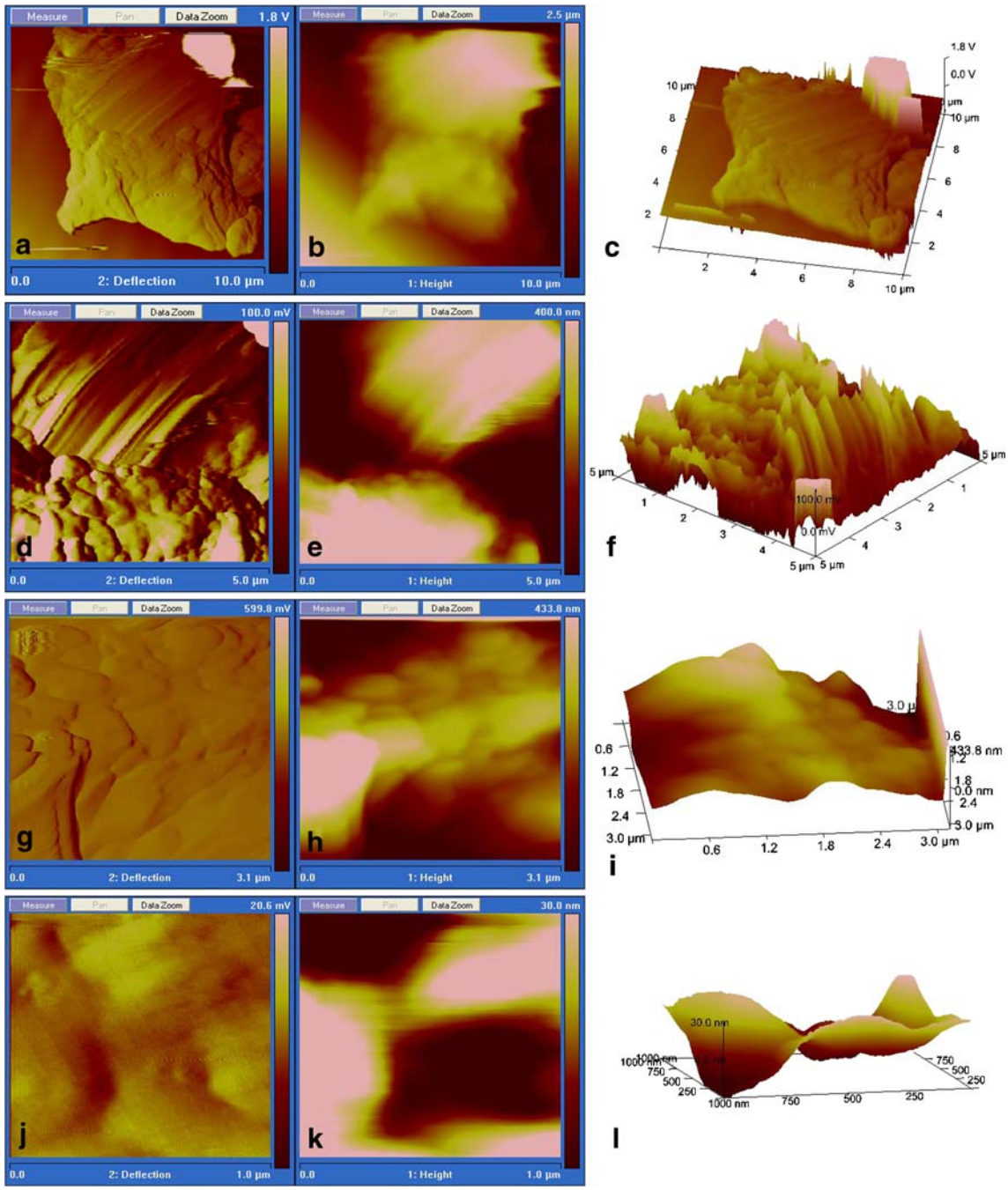

Fig. 4. AFM figures of batch 7 DCM: **a** deflection, **b** height, **c** 3D graph for 10 µm, **d** deflection, **e** height, **f** 3D graph for 5 µm, **g** deflection, **h** height, **i** 3D graph for 3.1 µm, **j** deflection, **k** height, **l** 3D graph for 1 µm

high polar solvent with hydrophobic surface as discussed earlier.

With batch 7, using DCM revealed a large concentric area of adsorbed drug with a considerable difference in the layout of adsorbed drug pattern, as seen in Fig. 4a. The large chunk of adsorbed drug area suggests the formation of stakes, thereby showing a large depth on all sides. On further magnification, the wavy nature becomes more prominent. The size of surface taken at 3×3 µm (Fig. 4g–i) and 1×1 µm (Fig. 4j–l) shows the layered form of adsorption phenomenon suggested by a number of counters with a stepwise formation. No cracks in the adsorbed drug pattern were observed, indicating its continuity over the surface. This supports the claim and explanation of interaction between the low polarity solvent DCM with the hydrophobic surface/pores on the adsorption pattern (24).

Porosity Data Evaluation

The drug-loading process influencing surface area and porosity was studied by adsorbing N_2 whose values are given (Table II). All isotherms were of type III showing hysteresis displayed due adsorption and desorption in mesopores (24). Using methanol, recorded values for all evaluation parame-

Table II. BET Values of Drug-Loaded Beads Using Different Adsorption Methods

	Surface area (m^2 /g)		Pore volume (cc/g)		Pore radius (Å)	
Batch	Methanol	DCM	Methanol	DCM	Methanol	DCM
1	4.016E+01	4.139E+01	1.656E−01	1.785E−01	8.741E+01	1.531E+02
2	2.867E+01	3.521E+01	5.773−03	1.4452E−01	8.727E+01	1.547E+02
3	3.254E+01	3.347E+01	5.117E−02	1.447E−01	8.706E+01	1.566E+02
4	2.994E+01	1.484E+01	8.862E−02	5.472E−02	8.792E+01	1.567E+02
5	3.626E+01	1.963+01	1.292−01	4.450E−02	8.800E+01	8.752E+01
6	3.996E+01	1.801E+01	1.425E−01	6.792E−02	8.719E+01	1.527E+02
7	2.951E+01	1.694E+01	9.135E−02	3.854E−02	8.730E+01	8.787E+01
8	2.874E+01	1.818E+01	7.586E−02	7.208E−02	8.718E+01	1.562E+02
9	2.201E+01	1.847E+01	4.988E−02	6.309E−02	8.805E+01	8.745E+01
A[a]	7.77E+01		1.98E−01		1.36E+01	

BET Brunauer–Emmett–Teller
[a] Accurel MP 1000®

ters showed influence of selected variables. With least solvent volume (1 ml), observed values decreased with increasing drug amount, which differed with increasing solvent volume irrespective of drug amount used. The reason for this can be attributed to the impact of variable solvent volumes, wherein capillary (at low-solvent volume) or pressure gradient (at high-solvent volumes leading to submerging) or both work in manipulating the adsorption pattern (26). This was evident from the graphs, which show increased activity below 50 Å with increasing solvent volume (supplementary data). However, batches using 200 mg drug showed high values using increased solvent volumes. This feature was not seen using mercury porosimeter, which followed a particular trend (12).

Using DCM, recorded values for all evaluation parameters showed varied patterns at different drug levels. Surface area decreased with increasing solvent volume at lowest amount of drug but with minor difference, which behaved oppositely at other two levels (200 and 300 mg). Negligible difference between the values was observed. This indicates the continuous adsorption pattern on the surface at increased drug amount where less/no accessibility of nitrogen gas was possible, thereby reconfirming our previous results. Once again, this sort of result was not obtained using mercury porosimetry.

Statistical interpretation of the data by regression analysis is given in Table III. Using methanol, observed values display a non-significant negative impact of drug–drug interaction (β^2) for surface area and positive drug interaction (β) for pore volume along with negative impact of drug–solvent ($\alpha\beta$) interaction. This distantly points toward the possibility of interactions of highly polar nature of solvent with drug containing both hydrophobic and hydrophilic groups on hydrophobic surface of Accurel MP 1000®. Using DCM, drug amounts (β) predict negative influence over surface area (Fig. 5a) and pore volume (Fig. 5b). The closely packed drug at the periphery of the surface may have hindered the nitrogen, thereby showing negative influence, while with methanol, the observed adsorption pattern must have worked conversely. Drug–drug interaction shows positive values for both response variables using DCM and negative response for surface area using methanol. This can be related to modified pore sizes and geometry after drug adsorption, which is more limited to outer surface using DCM and spread throughout using methanol.

Combined N_2 adsorption and mercury-intrusion porosimetry experiments on various porous materials have indicated a partial agreement concerning various aspects of evaluation parameters. Drug-loaded porous materials showed distinct difference and similarity of statistical data on comparing the present data with raw mercury porosimetry data conducted in our previous work. Values related to the amount of drug variable (β) showed its influence during MPA only while solvent–solvent interaction was absent for both. The difference between the analysis of mercury porosimetry data (12) and nitrogen sorption data can be correlated to the (a) different methodology basis of both techniques for their evaluation, (b) shape of individual pores after drug loading, (c) type of pore openings, (d) pore blockages, (e) relation between voids, and throat (f) the cooperative percolation effect of the porous network.

In vitro Drug Release

Basic theoretical background of drug release from hydrophobic porous polymeric system depends on (a) medium interaction (water) with surface, (b) drug dissolution in water-filled pores governed by pore volume and drug solubility, (c) diffusion through water-filled channels adopting least resistant channels, (d) geometry and structure of pore network based on contributing and non-contributing porosity, (e) physical and chemical interactions, (f) partitioning of the diffusant within the matrix wall, and (g) low drug loading leading to recovery. All these factors behave independently, opposite, or synergistically to increase or retard the mass transfer, thereby leading to the dissolution of drug influencing drug release (8,27–29).

The present drug delivery system somewhat resembles the air-enclosed system, which showed a maximum floating time of 9 h depending upon condition of stomach and supine position of the subject (30). Based on the position of subject (lying during night), working against the principle of gastro-retention, a floating study for 6 h was undertaken in pH 1.2 HCl IP medium maintaining sink conditions. All batches showed satisfactory floating characteristics during the time of experiment. This was followed by 3 h in pH 7.2

Table III. Estimation of Regression Coefficients for Different Response Variables

Coefficient	Response															
	Surface area		Pore volume		Burst release		Percent drug release (hours)									
							1		6		7		9			
	m	d	m	d	m	d	m	d	m	d	m	d	m	d		
C	26.35	13.02	0.094	0.052	49.59	47.06	3.791	1.383	23.10	10.00	73.86	59.29	76.42	66.86		
α	–	–	–	–	–	–	–0.978	–	–	–	–	–	–3.423	–5.05		
β	–	–7.518	0.015	–0.043	9.52	17.61	–1.30	1.6	–4.755	–1.32	5.05	16.296	6.476	17.12		
α^2	–	–	–	–	5.28	–	–	–	–	–	–	–	4.503	–		
β^2	–7.28	7.625	–	0.049	–	–	–	2.253	–3.781	3.343	–	–	–	10.44		
α β	–	1.29	–	–	–	–	1.33	–	–	–0.865	–	–	11.64	–		
R^2	0.3427	0.9923	0.1849	0.9460	0.8891	0.8398	0.7514	0.9354	0.9132	0.9149	0.4822	0.7720	0.8916	0.9261		
Sig.	0.0977	0.0000	0.2479	0.0002	0.0014	0.0005	0.0569	0.0003	0.0007	0.0042	0.0379	0.0018	0.0076	0.0029		

m methanol, *d* DCM

phosphate buffer IP taken as an appropriate dissolution medium to mimic increase in pH after floating. In our previous work, maximum impact of burst release occurred within 15 min followed by a very slow release or cutoff using basic medium for the same formulations (12). In present the formulation, being a multiparticulate system where there is no all-at-once emptying is noted, the analysis interval was set at 1 h after changing medium to normalize time for gastric emptying time and simultaneously the burst effect (13).

From Methanol Adsorbed Microparticles

Overall drug release show different release profiles, ranging 13–24% at the end of 6 h in acidic medium followed by the burst release with range of 41–68% to the previously released drug. The end release ranging 69–94% at 9 h is shown in Fig. 6. Release profile of all batches at the end of 6 h decreased with increasing amount of the drug used for adsorption with maximum intradifference using 3 ml. Increased surface area phenomenon along with contribution of open pores seizing more dissolution medium due to low drug amounts resulted in higher release rates. Batches with high drug amounts showed the least release irrespective of solvent volume used, which were nearly half or more than the starting least amount. Factors for this phenomenon can be related to (a) restricted/blocked surface, leading to low pore volume restricting mass transfer, (b) effect of low drug solubility in medium, (c) formation of multiple dissolution fronts, (d) roughness of surface, and (e) moment of dissolved drug packets from within the isolated or interconnected pores toward the dissolution medium. The flow and interaction of the dissolution medium inside the porous material appears to be critical in observing mass transfer. No significant difference in drug release was noted considering the same drug amount at different solvent volumes, indicating similar amount of drug amount ready for mass transfer.

Batch 6, with least release of 12.77% in acidic medium, shows significance in formulating the ideal system for chronotherapy favoring low release during gastroretentive period designated as lag period (Fig. 6b). The attainment of such release without using any release modifiers or subjecting to coating by single or multiple polymers or formulating in the form of simple or press-coated tablets or in the form of modified capsule consisting of various excipients makes it exceptional and lucid to formulate.

Statistical interpretations for the drug release were calculated at various time intervals, which was preferred over percent release as presented in Table III. The values conferred for the drug release in acidic medium show the negative impact of drug coefficient (β) throughout the time period. Initially, the negative solvent effect (α), along with positive solvent-drug ($\alpha\beta$) interaction, was noted, which vanish afterwards probably due to the behavior/dissolution of the outermost drug layer. The negative values of drug–drug (β^2) interaction up to half way indicate the dissolution of underlying drug layers from the surface influenced by adsorption pattern. These values suggest pronounced impact of drug coefficient at all levels irrespective of solvent volume.

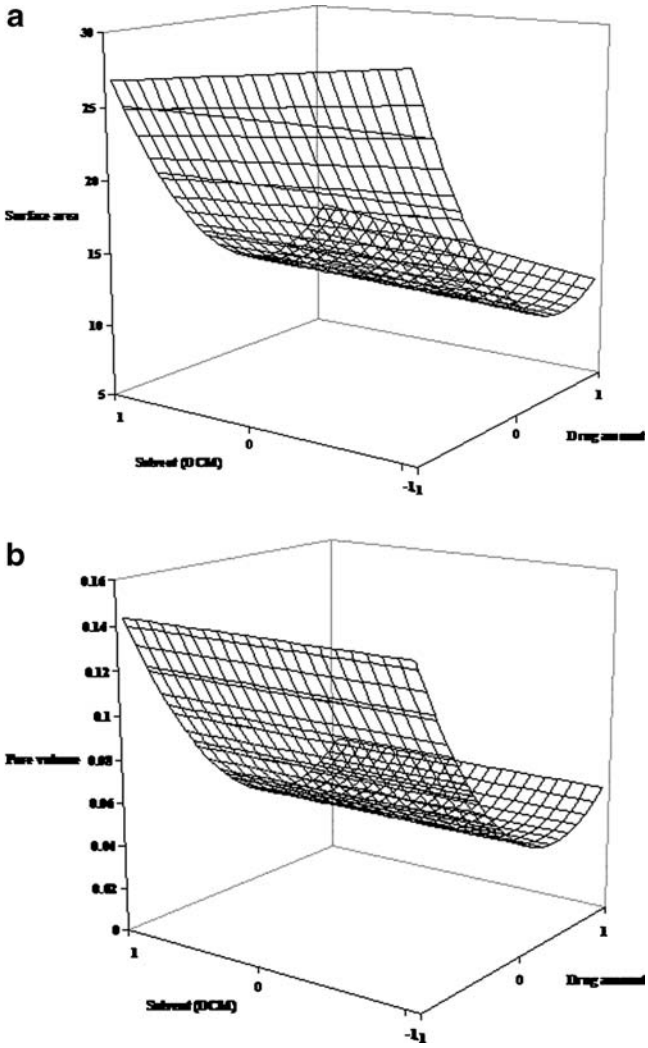

Fig. 5. Response surface plots showing effect of factorial variables on **a** surface area and **b** pore volume using DCM

Changing to phosphate buffer pH 7.2 IP initiated the sudden increase in release, with maximum burst release of 68.95% for batch 3. At the end of the experiment, batch 3 showed maximum release, while cut off was observed in some batches at 8-h mark. Sudden depletion of adsorbed drug clusters favors dominance of non-contributing porosity, thereby causing new boundary conditions. This leads to the exposure of underlying rough and hydrophobic nature of surface and pores to dissolution medium, which in turn assist in retarding/stopping the drug release. In other batches, slower drug release was observed after burst release was influenced by the continuity of adsorbed drug layer and its mass transfer momentum from inside to outside (29). Moving boundary conditions influencing geometry, described as Stephan moving problem (31,32), was perfectly observed in drug release while exposing porous carriers to basic medium alone than using acidic medium before it.

Statistically, drug as well as solvent–solvent (α^2) interaction coefficient showed a positive influence on burst release fraction (Fig. 7a), while a positive influence of drug coefficient (β) was observed at 7 h. The same observation at the end of experiment shows the contributions from most coefficients conferring the positive influences of the selected variables, which worked ambiguously in acidic medium. Inference from this illustrates the influence of dissolution medium favoring difference in drug solubility as in Fig. 7b. The positive values of drug coefficient suggest its effect in basic medium only. These types of influences were similar to our previous study where only basic medium was used (12).

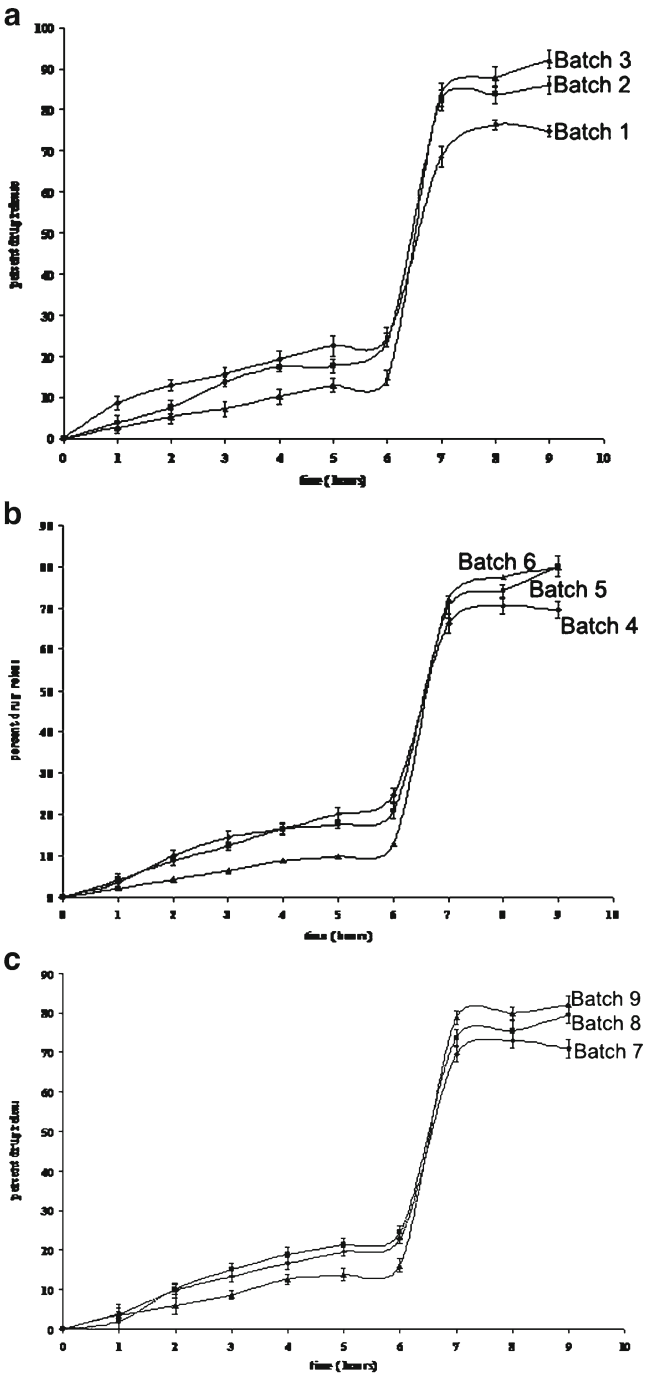

Fig. 6. Cumulative drug release profile from Accurel MP 1000 ® using methanol

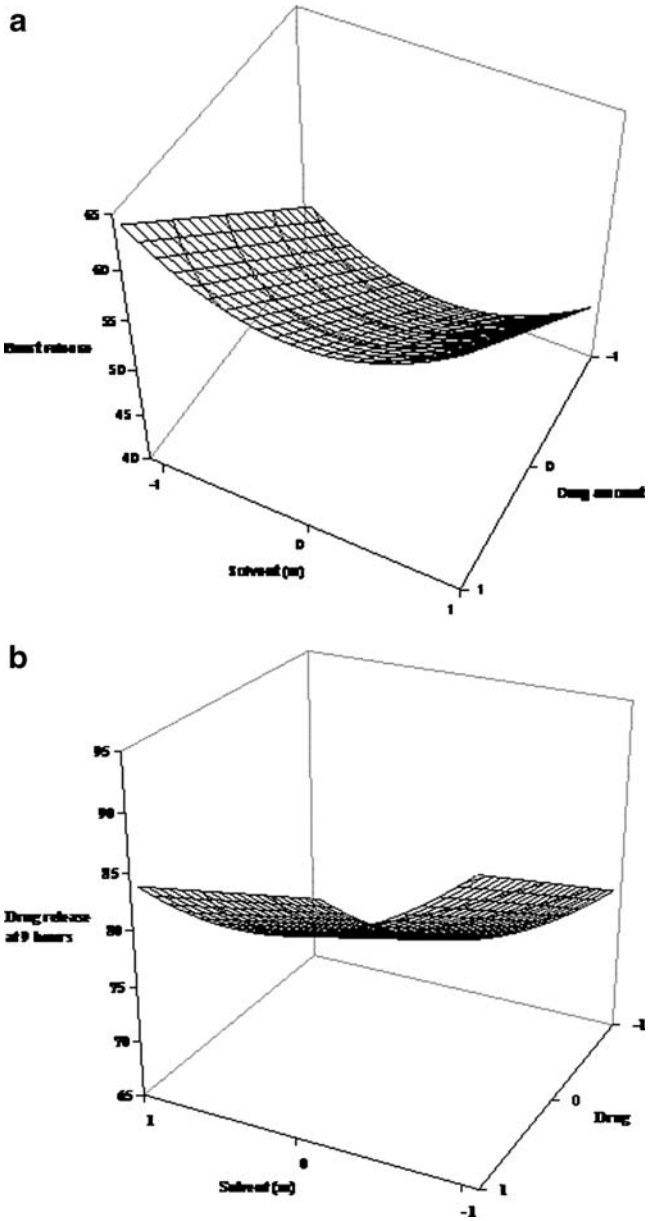

Fig. 7. Response surface plots showing the effect of factorial variables on **a** burst release **b** drug release at 9 h using methanol

Batch 3 can be considered as optimized formulation for the purpose of chronotherapy, with 14.79% release in acidic medium followed by burst of 68.95%. In addition, batch 6 can be preferred as the subsequent choice with 12.77% release in acidic medium followed by 58.05% burst release.

From DCM Adsorbed Microparticles

Overall, the drug release ranging 8–15% was much lower unlike corresponding methanol batches in acidic medium. Burst effect ranges 31–70%, and the final release range 55–99% was observed with a positive difference in some batches, as seen in Fig. 8. Factors governing the release pattern were more or less the same, probably differing in magnitude.

The release in acidic medium showed a characteristic trend recording the least release of batches using medium level of drug (200 mg) irrespective of solvent volume used. Batch 8 recorded the least release of 8%, as in Fig. 8c. This release is much lesser than any batch even from the methanol batches. The least/less drug release can be related to the ever decreasing pore volume caused by adsorption of drug

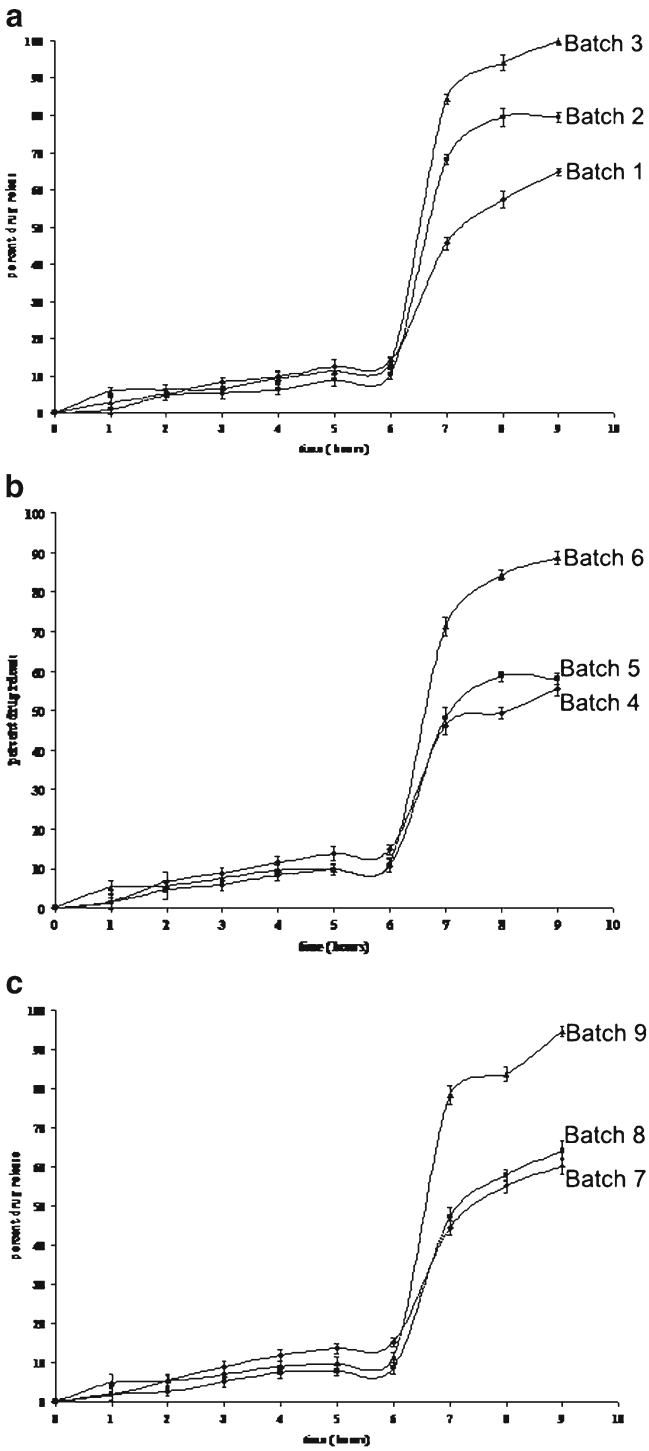

Fig. 8. Cumulative drug release profile from Accurel MP 1000® using DCM

influenced by solvent property. This again supports the adsorption pattern of drug at meniscus of porous material using less polar solvent (24). The influence of the different solvent volume was not evident in acidic medium. Statistical interpretation show negative influence of drug (β) but a positive influence of drug–drug interaction (β^2), as in Fig. 9a. This can be due to the development of various adsorption patterns in the form of stakes, which influence inter-pore connective influencing pore volume.

Burst release fraction, on changing to basic medium, observed increased release with increasing drug amount. It was twice or more for all solvent volumes used. The main feature, as shown by DCM, was the high burst release fraction for batch 3 at 70%. The less burst release in batch 1(lowest drug amount) can be due to fast exposure of underlying hydrophobic pores and surface, thereby retarding the drug release. These effects seem to be nullified with increasing amount of drug used for adsorption, where the adsorbed drug clusters act as the reservoirs for increased drug release. This difference can be summed up for the interaction

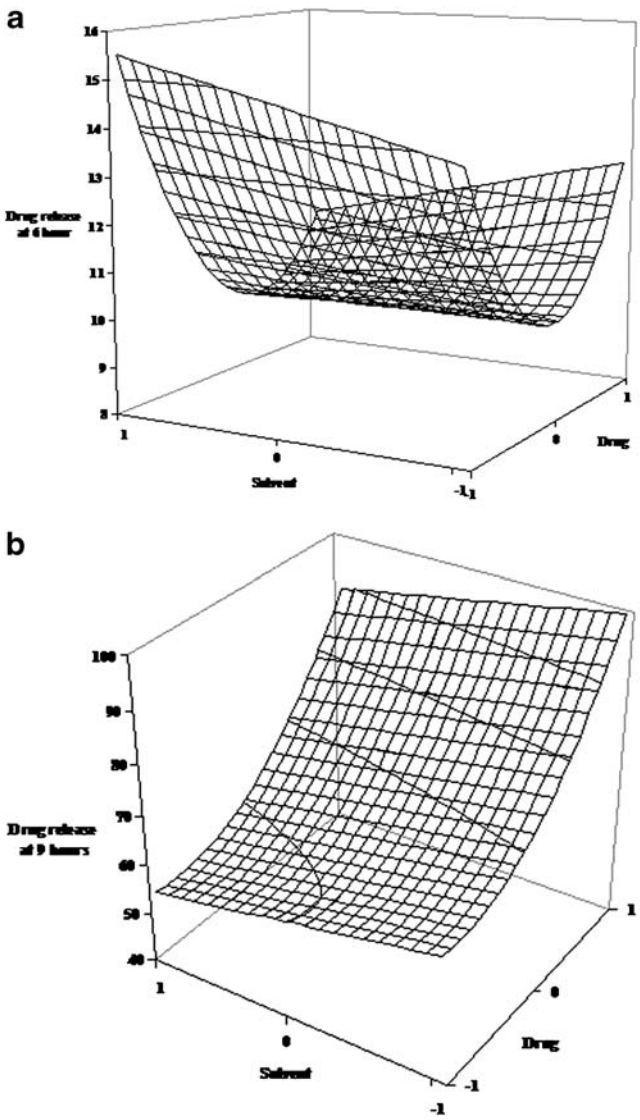

Fig. 9. Response surface plots showing effect of factorial variables on **a** drug release at 6 h, **b** drug release at 9 h using DCM

of the nature of solvents and mediums affecting drug adsorption leading to the different rate mass transfer. Positive drug coefficient influence was observed statistically, which did not change when clubbed with total drug release for 7 h.

At the end of the experiment, batch 3 showed maximum release the same as that of methanol. Comparing with methanol batches, better drug release was observed using maximum drug amount, while a lesser drug release was calculated for other drug amounts. This can be due to variable mass transfer caused by boundary conditions of the adsorbed drug layer.

Statistically, at the end of the experiment, positive contributions from drug variables were prominent along with negative effect of solvent characteristic of solvent nature, as in Fig. 9b.

Overall, again, batch 3 can be considered as the most optimized formulation for effective floating pulsatile drug delivery with 13.48% release in acidic medium followed by burst of 70.91%. In addition, batch 9 can be preferred as the subsequent choice with 11.34% drug release in acidic medium and 66.95% as burst release.

Stability studies predict no significant changes in the drug release. Apart from this, DSC and XRD show the same results with marginal difference.

CONCLUSION

A lucid and simple floating pulsatile drug delivery system intended for chronotherapy was achieved using 3^2 factorial design for optimizing the formulation. Single-step adsorption techniques, unaided by additives, are promising enough for further evaluation of present and various other drug delivery systems. Using this process, four different batches with desired release parameters can be selected. BET and mercury data seem to behave differently in accordance with the principle of instrument working. Cross-sections predicted the inner core geometry of adsorbed porous carrier giving an insight about the possible drug release phenomenon. The modified geometry and network structure of pores in Accurel MP 1000® due to influence of selected variables govern the desired drug release pattern. The dissolution medium showing varying drug solubility shows multiple variations in pore volume and pore surface, therefore affecting porosity and permeability. Variable effect was dormant in acidic medium. This influenced the drug release rate process, which in turn is also dependent on static and changing adsorbing pattern of drugs. This work can be extended for time-scheduled drug release of drugs having low solubility, poor absorption, or degradation in lower gastrointestinal tract.

ACKNOWLEDGMENTS

Praveen Sher is thankful to Dr. James R. Benson of Polygenetics, Inc. for his valuable advice during work. Praveen Sher and Atmaram Pawar are also thankful to UGC, India for providing major research project. Authors are thankful to Dr. Smita Mule (DSC), A.B. Gaikward (SEM), Baishakhi (AFM), and Supriya Palimkar for help in evaluation work. Authors also thank Membrana, Germany for providing a free gift sample of Accurel MP 1000®, particularly Ms. Claudia Gramann for her support.

REFERENCES

1. Andersson J, Rosenholm J, Areva S, Linden M. Influences of material characteristics on ibuprofen drug loading and release profiles from ordered micro- and mesoporous silica matrices. Chem Mater 2004;16:4160–7.
2. Shivanand P, Sprockel OL. A controlled porosity drug delivery system. Int J Pharm 1998;167:83–96.
3. Li Z, Wen L, Shao L, Chen J. Fabrication of porous hollow silica nanoparticles and their applications in drug release control. J Control Release 2004;98:24–254.
4. Song S-W, Hidajat K, Kawi S. Functionalized SAB-15 material as carrier fro controlled drug delivery: influence of surface properties on matrix–drug interactions. Langmuir 2005;21:9568–75.
5. Salonen J, Laitinen L, Kaukonen AM, Tuura J, Bjorkqvist M, Heikkila T, Vaha-Heikella K, Hirvonen J, Lehto V-P. Mesoporous silicon microparticles for oral drug delivery: loading and release of five model drugs. J Control Release 2005;108:362–74.
6. Ohta KM, Fuji M, Takei T, Chikazawa M. Development of a simple method for the preparation of a silica gel based controlled drug delivery system with a high drug content. Eur J Pharm Sci 2005;26:87–96.
7. Otsuka M, Tokumitsu K, Matsuda Y. Solid dosage form preparations from oily medicines and their drug release. Effect of degree of surface modification of silica gel on the drug release from phytonadione-loaded silica gels. J Control Release 2000;67:369–84.
8. Streubel A, Sipeman J, Bodmeier R. Floating microparticles based on low density foam powder. Int J Pharm 2002;241:279–92.
9. Streubel A, Sipemann J, Bodmeier R. Multiple unit gastroretentive drug delivery systems: a new method for low density microparticles. J Microencapsul 2003;20(3):329–47.
10. Li Y-h, Zhu J-b. Modulation of combined-release behaviors from a novel "tablets-in-scapsule system". J Control Release 2004;95 (3):381–9.
11. Gren T, Bjerre C, Camber O, Ragnarsson G. *In vitro* drug release from porous cellulose matricies. Int J Pharm 1996;141:53–62.
12. Sher P, Ingavle G, Ponrathnam S, Pawar AP. Low density porous carrier: drug adsorption and release study by response surface methodology using different solvents. Int J Pharm 2007;331:72–83.
13. Sher P, Ingavle G, Ponrathnam S, Pawar AP. Low density porous material based conceptual drug delivery system. Microporous Mesoporous Mater 2007;102:290–8.
14. Stubbe BG, Smedt S, Demeester CD. Programmed polymeric devices for pulsed drug delivery. Pharm Res 2004;21:10.
15. Badve SS, Sher P, Korde A, Pawar AP. Development of hollow/porous calcium pectinate beads for floating pulsatile drug delivery. Eur J Pharm Biopharm 2007;65:85.
16. Lee B-J, Min G-H. Oral controlled release of melatonin using polymer-reinforced and coated alginate beads. Int J Pharm 1996;144(1):37–46.
17. Lee B-J, Ryu S-G, Cui J-H. Controlled release of dual drug-loaded hydroxypropyl methylcellulose matrix tablet using drug-containing polymeric coatings. Int J Pharm 1999;188 (1):71–80.
18. Bussemer T, Bodmeier R. Formulation parameters affecting the performance of coated gelatin capsules with pulsatile release profiles. Int J Pharm 2003;267(1–2):59–68.
19. Dashevsky A, Mohamad A. Development of pulsatile multiparticulate drug delivery system coated with aqueous dispersion Aquacoat® ECD. Int J Pharm 2006;318(1–2):124–31.
20. Efentakis M, Koligliati S, Vlachou M. Design and evaluation of a dry coated drug delivery system with an impermeable cup, swellable top layer and pulsatile release. Int J Pharm 2006;311 (1–2):147–56.
21. Ravishankar H, Patil P, Samel A, Petereit H-U, Lizio R, Iyer-Chavan J. Modulated release metoprolol succinate formulation based on ionic interactions: *in vivo* proof of concept. J Control Release 2006;111(1–2):65–72.
22. Gunko VM, Mikhalovskii SV, Melillo M, Voronin EF, Nosach LV, Pakhlov EM. The effect of the nature and structure of adsorbents on interaction with ibuprofen. Theor Exp Chem 2004;40(3):137–43.
23. Janczuk B, Chibowski E, Wojcik W. The influence of n-alcohols on the wettability of hydrophobic solids. Powder Technol 1985;45:1–6.
24. Sarkisov L, Monson PA. Modeling of adsorption and desorption in pores of simple geometry using molecular dynamics. Langmuir 2001;17:7600–4.
25. Scott DC. An assessment of reasonable tortuosity values. Pharm Res 2001;18(12):1797.
26. Germann PF, DiPietro L. When is porous-media flow preferential? A hydromechanical perspective. Geoderma 1996;74:l–21.
27. Faruk C. Scale effect on porosity and permeability: kinetics, model and correlation. AIChE J 2001;47(2):271–87.
28. Tongta A, Liapis AI, Siehr DJ. Equilibrium and kinetic parameters of the adsorption of a -chymotrypsinogen A onto hydrophobic porous adsorbent particles. J Chromatogr A 1994;686:21–9.
29. Siegel RA, Kost J, Langer R. Mechanist studies of macromolecular drug release from macroporous polymers. I experiments and preliminary theory concerning completeness of drug release. J Control Release 1990;8:223–36.
30. Iannuccelli V, Coppi G, Sansone R, Ferolla G. Air compartment multiple-unit system for prolonged gastric residence. Part II. *In vivo* evaluation. Int J Pharm 1998;174:55–62.
31. Collins R. Mathematical modeling of controlled release from implanted drug-impregnated monoliths. Pharm Sci Technol Today 1998;1(6):269.
32. Collins R, Jinuntuya N, Petpirom P, Wasuwanich S. Mathematical model for controlled diffusional release of dispersed solute drugs from monolithic implants. Ann N Y Acad Sci 1998;858:116.